

NON DESTRUCTIVE TESTING TECHNIQUES FOR RISK BASED INSPECTION

F. Van den Abeele¹ and P. Goes¹

¹ OCAS N.V., J.F. Kennedylaan 3, 9060 Zelzate, Belgium

Abstract

Ensuring the safety of offshore structures is of vital importance for the reliability of oil and gas drilling rigs. Risk based inspection (RBI) is becoming an industry standard for management of equipment integrity. The objective of risk based inspection is to determine the likelihood of equipment failure (probability) and the consequences of such an event. Combining the probability of an event with its possible consequences allows determining the risk of an operation. Risk based inspection enables to optimize the frequency of inspection, by moving from periodic inspection (based on arbitrary calendar dates) to an informed inspection program (based on equipment condition).

One of the most important tools to determine the condition of the equipment, and to calculate its reliability, is the use of non destructive testing (NDT) techniques to detect cracks, flaws and defects. The probability of detection and the probability of sizing depend on the type of NDT method used. Combining NDT information on crack size and depth with fracture mechanics based damage models, allows predicting the remaining life time of a component.

In this paper, the philosophy of risk based inspection is introduced and recent advances in non destructive testing (in particular ultrasonic and electromagnetic techniques) are reviewed. Then, the use of fracture mechanics based damage models is demonstrated to predict fatigue failure for offshore structures.

Keywords inspection, reliability, non destructive testing, ultrasonics, ACFM, structural integrity, risk

1 PHILOSOPHY OF RISK BASED INSPECTION

The objective of Risk Based Inspection (RBI) is to determine what incident could occur (*consequence*) in the event of an equipment failure, and how likely (*probability*) it is that the incident could happen. Multiplying the likelihood of an incident with its possible consequences will determine the *risk* associated to the operation.

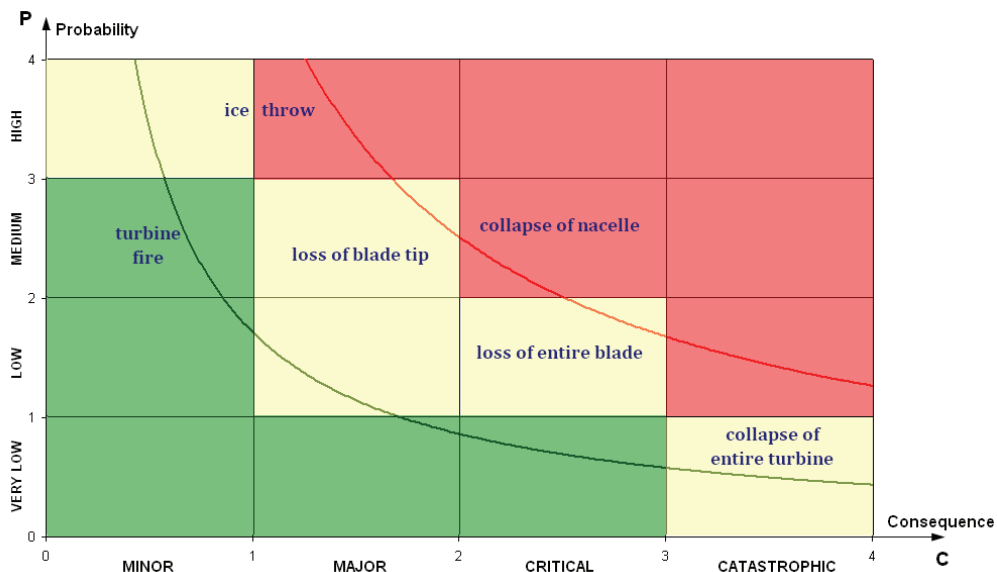


Figure 1: Criticality matrix for risks associated with the installation of wind turbines

In a qualitative risk assessment, the combination of probability and consequence can be visualized in a *criticality matrix*. On Figure 1, such a scheme is presented to evaluate the environmental risks associated with the installation of large (≥ 2 MW) wind turbines.

Some failures may occur frequently, but without significant adverse impacts. Similarly, other failures can have potentially serious consequences, but if the probability of the incident is low, than the resulting risk may not warrant immediate action. If the risk is medium, mitigation measures are normally subject to a cost/benefit analysis. Action will be taken if the cost of implementing the measure is lower than the loss, associated with the possible event. When the risk is not acceptable, mitigation measures have to be put in place.

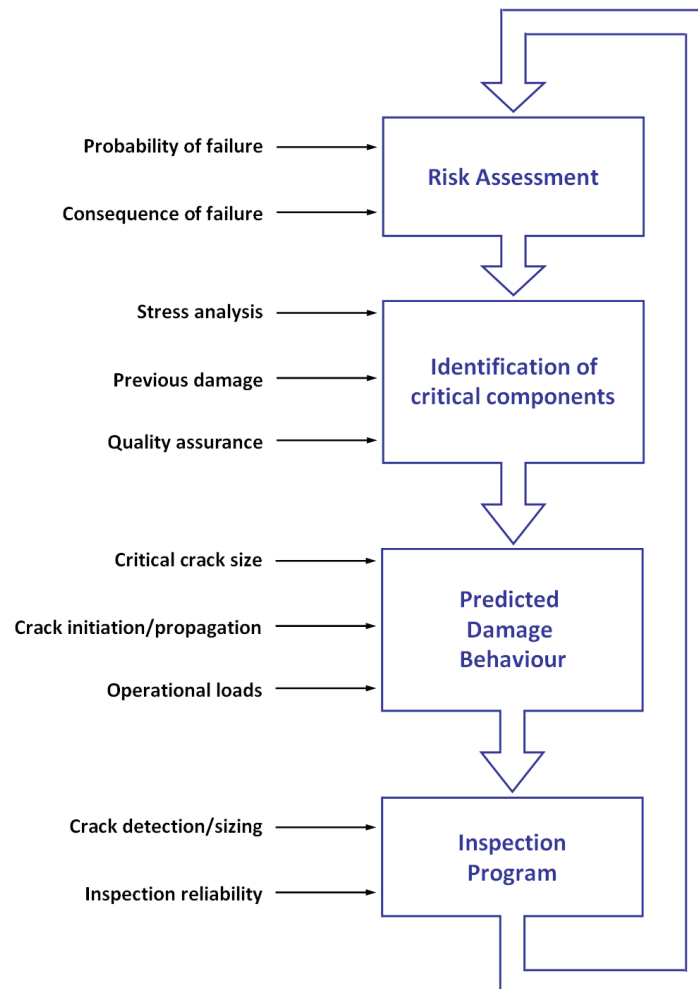


Figure 2: Flowchart for Risk Based Inspection program

As shown on the flowchart, the risk assessment (either qualitative or quantitative) is used as an input to determine the inspection interval for an RBI maintenance program. The aim is to deploy a finite inspection resource according to a ranked list of components and their associated level of risk. In that respect, risk based inspection enables to optimize the frequency of inspection, by moving from period inspection (based on arbitrary calendar dates) to an informed inspection program (based on equipment condition).

Indeed, the hazard rate of most engineering equipment follows a so-called *reliability bath tub curve*, shown on Figure 3, which is characterised by three distinct regions. The first region corresponds to the start of life, and an increased hazard rate due to variation in material properties and strength, poor design, manufacturing defects and human errors during installation and operation. As a result, most weak items fail during this phase causing a decrease of the initially high hazard rate.

The second region (useful life) is characterised by an approximately constant hazard rate. Failures in this region are not due to age, wear-out or degradation and preventive maintenance does not affect the hazard rate. The third region is characterized by an increased hazard rate due to wear-out and degradation of properties. Figure 3 shows how a profound understanding of these governing failure mechanisms allows optimizing the inspection intervals.

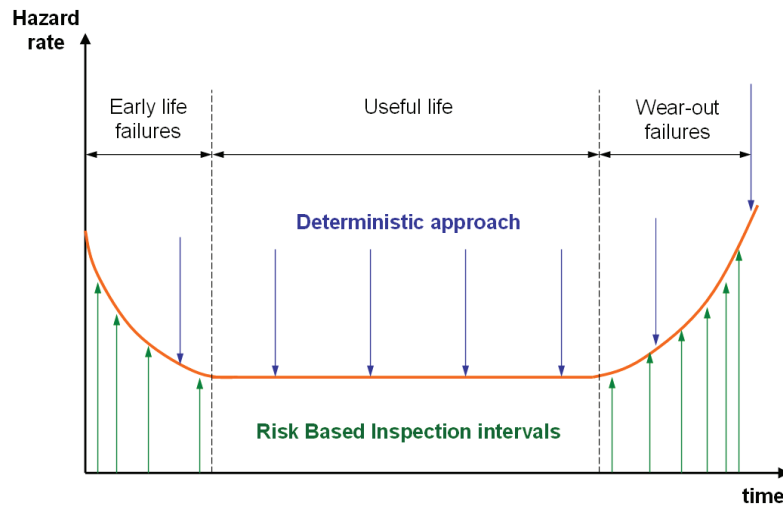


Figure 3: Reliability bathtub curve

It can be demonstrated [8] that the three regions of the bathtub curve can be described by a two parameter Weibull distribution

$$F(t) = 1 - \exp \left[- \left(\frac{t}{\eta} \right)^m \right] \quad (\text{Eq. 01})$$

which gives the probability that failure will occur before time t for a characteristic life time η and a shape parameter m . The reliability is, by definition,

$$R(t) \equiv 1 - F(t) = \exp \left[- \left(\frac{t}{\eta} \right)^m \right] \quad (\text{Eq. 02})$$

Differentiating (Eq. 01) with respect to time yields the probability density function

$$f(t) = \frac{m}{\eta} \left(\frac{t}{\eta} \right)^{m-1} \exp \left[- \left(\frac{t}{\eta} \right)^m \right] \quad (\text{Eq. 03})$$

and the corresponding hazard rate can be calculated as

$$h(t) = \frac{f(t)}{R(t)} = \frac{m}{\eta} \left(\frac{t}{\eta} \right)^{m-1} \quad (\text{Eq. 04})$$

which is plotted on Figure 3 for different values of the shape factor m . The hazard rate $h(t)$ is decreasing for $m < 1$ and increasing for $m > 1$, while the $m = 1$ corresponds to a constant hazard rate. Hence, a Weibull probability distribution (Eq. 01) with a shape factor $m < 1$ indicates early-life failures, whereas $m > 1$ describes wear-out failures. Values in the interval $[1 < m < 4]$ typically indicate early wear-out failures caused by low cycle fatigue, corrosion or erosion. Old age wear-out can be described by higher values of the shape factor ($m > 4$). For $m = 1$, the Weibull distribution (Eq. 01) transforms into the negative exponential distribution

$$F(t) = 1 - \exp(-\lambda t) \quad (\text{Eq. 05})$$

with $\lambda = 1/\eta$, which describes the useful region of the bath-tub curve, where the probability of failure within a specified time interval does not depend on age. During the useful life, the hazard rate is constant, i.e.

$$h(t) = \lambda = \frac{1}{\eta} \quad (\text{Eq. 06})$$

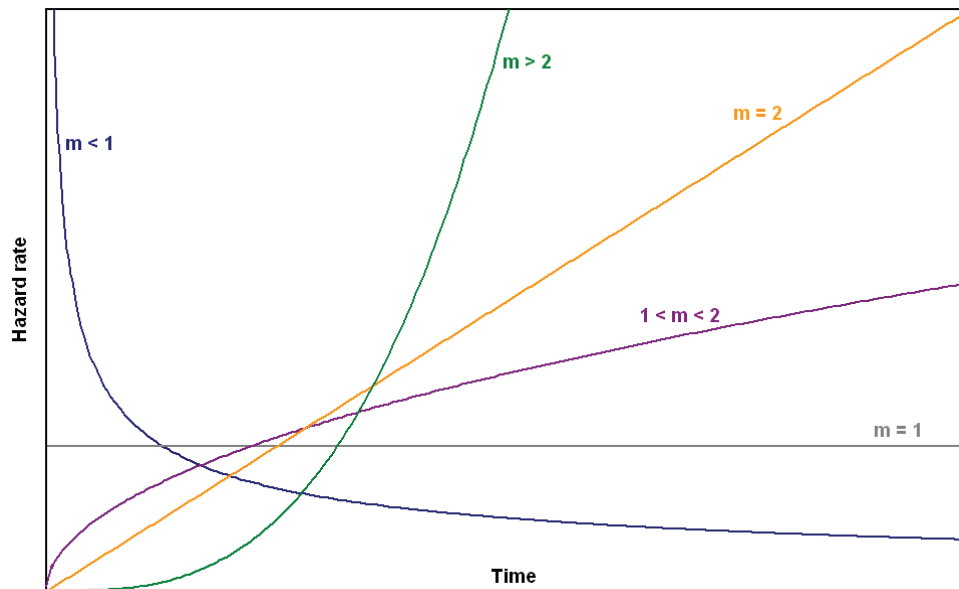


Figure 4: Weibull hazard rate for different values of the shape factor m

As evident from the reliability bathtub curve in Figure 3, and the flowchart on Figure 2, the effectiveness of an RBI inspection interval depends on

- **The ability to monitor equipment condition.** For processing plants, petrochemical equipment and offshore structures, non destructive testing (NDT) is the preferred technique to evaluate the integrity of pressure vessels, pipelines, tubular joints, underwater welds, piping,... In the next section, some recent advances in non destructive testing (in particular ultrasonic and electromagnetic techniques) are reviewed that enable a more accurate condition monitoring.
- **The inspection reliability.** The probability of detection (POD) is a statistical measure of the success of an inspection, whereas the probability of sizing (POS) provides an indication of sizing accuracy. Both POD and POS depend on the type of NDT method used. In section 3, the implications of probability of detection and sizing on an RBI program are briefly discussed.
- **Prediction of the remaining life time.** Combining NDT information on crack size and depth with damage models allows predicting the remaining life of a component. At the end of this paper, fracture mechanics is applied to estimate the fatigue life of a cracked component, taking into account the inspection reliability.

2 RECENT ADVANCES IN NON DESTRUCTIVE TESTING

The offshore industry has been aware of the need for an understanding of the performance of the NDT systems used in crack detection and sizing for quite some time [2]. A large number of offshore structures consist of steel welded tubular joints, like shown on Figure 5, the better part of which are underwater. Such nodal joints can be highly stressed and subjected to cyclic loading, which makes them vulnerable to fatigue failure.

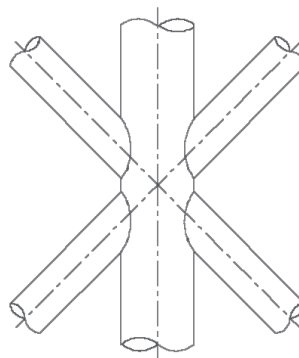


Figure 5: Welded tubular joint

An undetected fatigue crack caused the Alexander Keilland to disaster [3] in 1980. The capsizing was the worst disaster in Norwegian waters since the second World War, and clearly stresses the importance of underwater inspection. A review of the early developments in diver inspection and the maturation of subsea NDT technologies is given in [4], while [5-6] address the role of non destructive testing in the offshore industry. A comprehensive overview of non destructive testing for the offshore industry is presented in [7]. In this section, some recent advances in ultrasonic testing and electromagnetic NDT techniques are briefly described.

2.1 Ultrasonic non destructive evaluation

Ultrasonic inspection is based on elastic wave propagation and detection. For an intact homogeneous material, the sound path is straight and the wave velocity is constant. Flaws in the material will cause refracted sound waves. The pulse-echo technique, shown on Figure 6, is the most commonly used ultrasonic method for offshore inspection. A transducer/receiver (T/R) probe is acoustically coupled to the specimen and generates an incident sound pulse P. When a flaw is present, the refracted signal F will appear on the oscilloscope before the back wall echo E. The time of flight is an indication of the position of the crack. In addition, time of flight diffraction (TOFD) methods can be used to estimate the crack size.

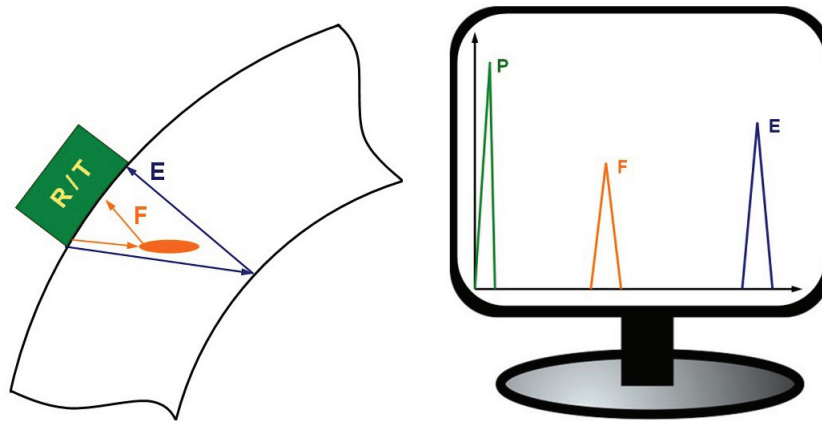


Figure 6: Pulse-echo technique for a tubular joint

In [8-9], ultrasonic bounded beam interactions are study features of the object under investigation. An incident bounded beam is modelled as a Fourier series of plane ultrasonic waves

$$\phi(x, z, t) = \frac{\exp(-i\omega t)}{2\pi} \int_{-\infty}^{+\infty} A(k_x) \exp[i(k_x x + k_z z)] dk_x \quad (\text{Eq. 07})$$

where the amplitude function can be written as

$$A(k_x) = \int_{-\infty}^{+\infty} F(\tau) \exp(-i k_x \tau) d\tau \quad (\text{Eq. 08})$$

where the components $\{k_x, k_z\}$ of the wave vector are connected to the angular frequency ω and the acoustic wave velocity c through

$$k_x^2 + k_z^2 = \left(\frac{\omega}{c}\right)^2 \quad (\text{Eq. 09})$$

and

$$f(\tau) = \exp(-\tau^2) \quad (\text{Eq. 10})$$

for a Gaussian beam. It is demonstrated [9-10] that the reflected (and transmitted) beam, like schematically shown on Figure 7, are a fingerprint of the structure under investigation, and can reveal (sub)surface features.

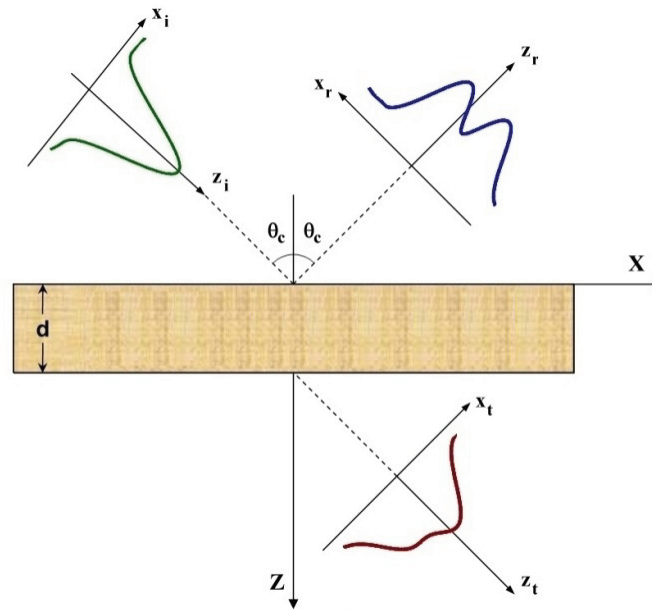


Figure 7: Ultrasonic bounded beam interactions to reveal subsurface features

More recently, phased array techniques have been developed and introduced as enhanced ultrasonic non destructive testing methods. Phased array technology is the ability to modify electronically the acoustic probe characteristics, by introducing time shifts in the signals sent to (pulse) and received from (echo) individual elements of an array probe [11]. Accurate time delays allow constructive and destructive interference, and permit complex inspections including beam steering, electronic scanning and dynamic depth focusing. Details on the use of ultrasonic phased array techniques for crack detection and sizing of defects can be found in [11-12].

2.2 Electromagnetic techniques

In addition to ultrasonic non destructive testing, a number of electromagnetic techniques is available, ranging from magnetic particle inspection over eddy current testing up to potential drop measurements. The working principles of these testing techniques, and their merits and limits for offshore inspection have been covered in [7]. In this paper, we will focus on the more recent developments: Alternating Current Potential Drop (ACPD) and Alternating Current Field Measurements (ACFM).

When alternating current with (angular) frequency ω is passed through a conductive media with conductivity σ and (absolute) magnetic permeability μ , the current will flow in a thin layer on the outer surface with skin depth

$$\delta = \sqrt{\frac{1}{\sigma \mu \omega}} \quad (\text{Eq. 11})$$

This skin effect is the main advantage of the Alternating Current Potential Drop (ACPD) method: the required power source is limited, and the crack disturbs a significant percentage of the total flow path, resulting in an enhanced accuracy. The ACPD method allows estimating the crack depth

$$d = \frac{\Delta}{2} \left(\frac{V_c}{V_r} - 1 \right) \quad (\text{Eq. 12})$$

like schematically shown on Figure 8. The method requires little or no calibration and provides a straightforward interpretation of crack depth. On the other hand, electrical contact is still required, so the structure has to be cleaned to bare metal.

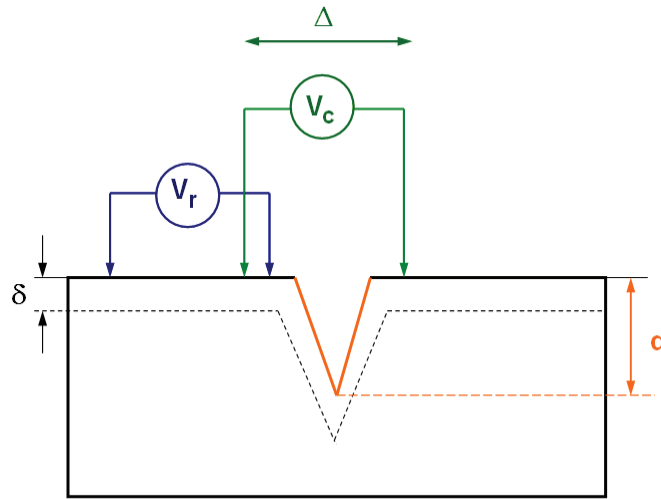


Figure 8: Alternating Current Potential Drop

The Alternating Current Field Measurement (ACFM) technique was developed for offshore applications [13] to maintain the advantages of ACPD while avoiding its limitations. This is achieved by injecting a uniform incident current, measuring the magnetic field components and relating them to the surface electric field. The ACFM sensor consists of two air wound coils, sensitive to changes in the B_x and B_z fields, which are parallel and normal to the crack respectively. With uniform current flowing in the y -direction and no defects present, $B_z = 0$ and B_x is uniform.

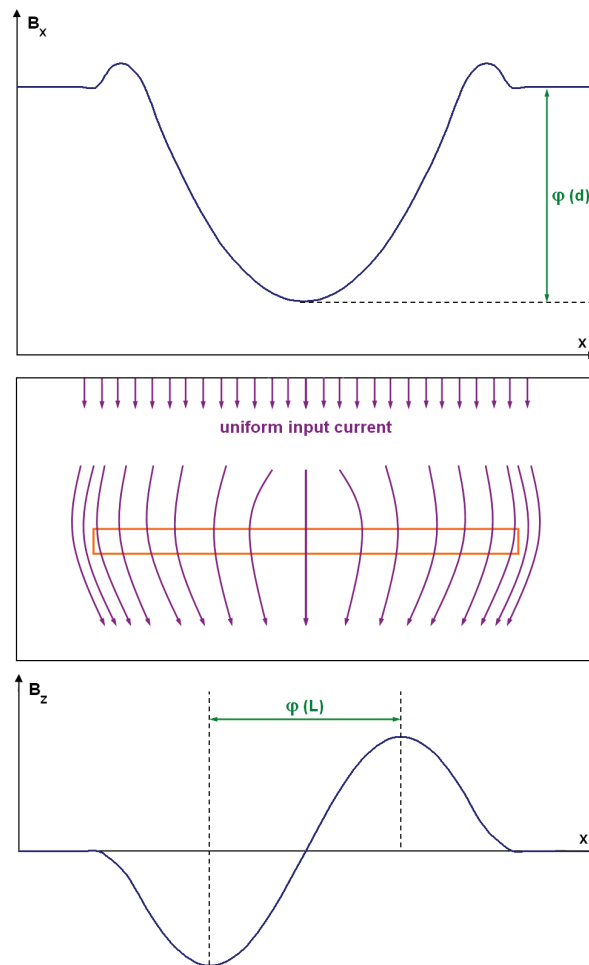


Figure 9: Alternating Current Field Measurements

The presence of a surface discontinuity diverts the current away from the deepest part and concentrates it near the ends of the defect. This produces a strong peak in the B_z signal near the ends of the crack, while the B_x signal drops in strength. As a result, the B_x signal contains information about the depth of the defect, while B_z is a measure for the crack length. The B_y signal is similar to B_z , but can be measured to distinguish between a crack and a pit. More details on the electromagnetic modelling to relate the field components to the dimensions of the defect can be found in [7].

The Alternating Current Field Measurement technique was originally developed for manual inspection of offshore welds, but is now available for use in many applications where reduced cleaning and inspection through coatings is a benefit [14-16]. The technique does not require contact, can cope with marine fouling and coatings, enables crack sizing (depth and length) and allows for considerable cost savings [17].

3 PROBABILITY OF DETECTION AND PROBABILITY OF SIZING

Although Alternating Current Field Measurements and ultrasonic phased array techniques provide innovative means of non destructive evaluation, the accuracy of the RBI program still depends on the inspection reliability. The inspection data should reveal the location of a defect, and the length and depth of the crack. The probability of detection (POD) is a statistical measure of the success of an inspection, whereas the probability of sizing (POS) provides an indication of sizing accuracy. In this section, the implications of POD and POS on an RBI program are briefly discussed.

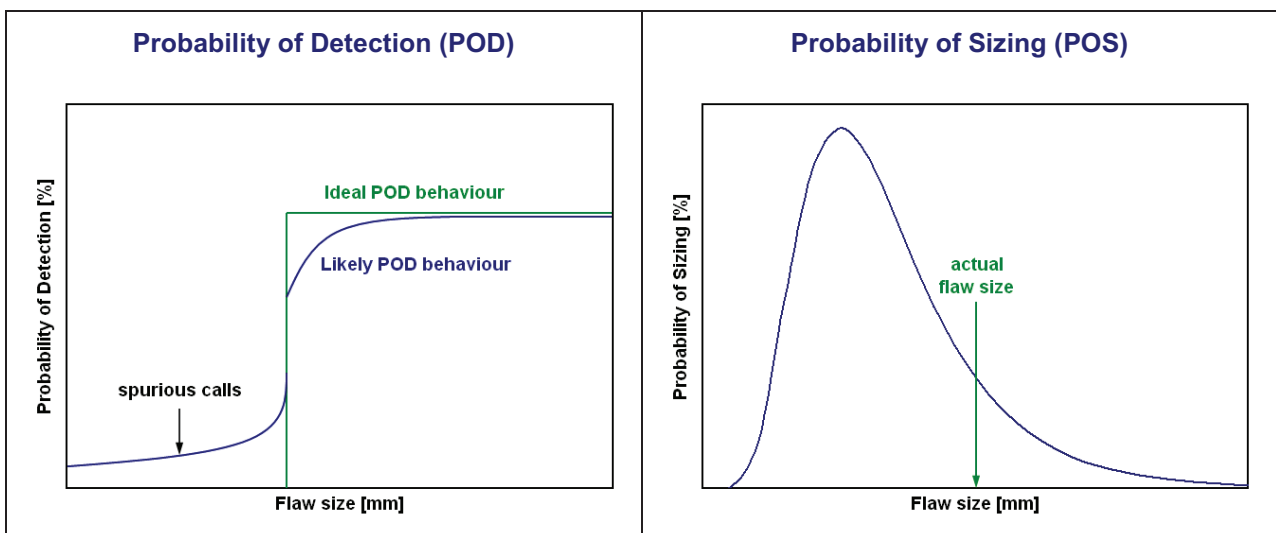


Figure 10: Probability of Detection (POD) and Probability of Sizing (POS)

3.1 Probability of Detection

The probability of detection (POD) is a statistical measure of the success of inspection, which can be expressed as a function of flaw size (like shown on Figure 10). A measured POD curve is obtained from the result of blind inspection trials, involving a range of defects in representative components and environments. Indeed, it is not possible to consider the performance of an NDT method on *all* cracks that may exist (i.e. the entire population). Instead, a sample must be chosen which is representative of the population. The confidence that the measured POD is representative of the population is dependent on the sample size. Assuming independent trials, the binomial distribution

$$P(S) = \frac{N!}{S!(N-S)!} p^s (1-p)^{(N-S)} \quad (\text{Eq. 13})$$

is valid, and the confidence that the measured POD is representative of the population can be estimated as [18]

$$C = 1 - p^N \quad (\text{Eq. 14})$$

which provides an elegant means of determining the minimum sample set required to reach a given confidence level [19].

3.2 Probability of Sizing

Probability of sizing (POS) is a measure of a particular inspection method's ability to accurately quantify the dimensions of a flaw or defect. The reliability of ultrasonic NDT methods to inspect pipelines used in the oil industry is covered in [20], and a similar analysis for the ACFM technique is presented in [21]. An example of a POS distribution is shown on Figure 10, for a non destructive testing method which is bound to under-predict the actual flaw size. Hence, this inspection method is likely to be un-conservative. This information has to be incorporated in the damage predictions, like presented in [19] and explained in the next section.

4 FATIGUE CRACK GROWTH PREDICTIONS FOR OFFSHORE STRUCTURES

In order to evaluate whether or not a (detected) crack is critical, the design engineer has to understand the ability of a structure to resist further damage, and the critical amount of damage that the structure can sustain before remedial action is required. Standards and codes like [22] and [23] were developed for pressure vessels and carbon steel pipes, and can be used for defect assessment of offshore structures as well. These codes use fracture mechanics based damage models to predict crack growth and the remaining life of the structure. However, relatively small errors in initial flaw size could have very large consequences on the predicted remaining life. Therefore, it is important to introduce the inspection reliability in the calculations. The application of POD data in the prediction of corrosion rates for offshore pipelines has been presented in [19]. Here, the influence of probability of detection and probability of sizing on fatigue crack growth calculations is demonstrated.

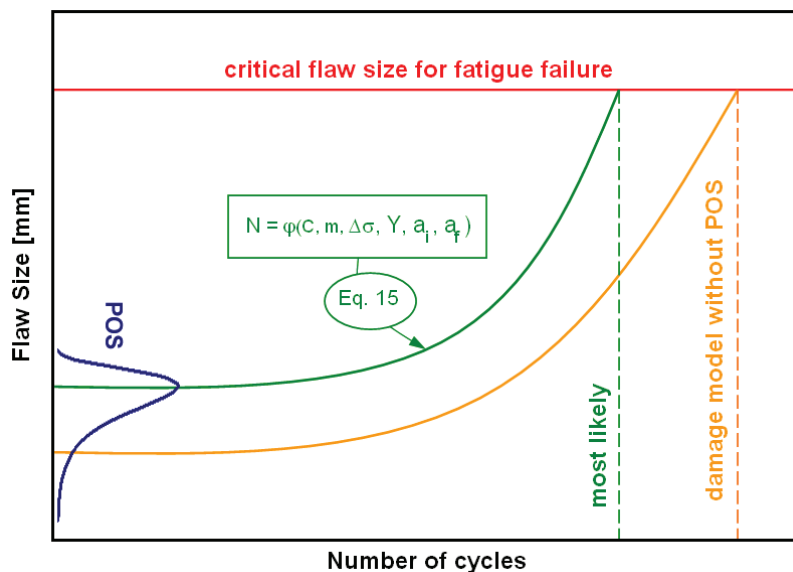


Figure 11: Prediction of fatigue crack propagation using inspection reliability data

In linear elastic fracture mechanics, the fatigue growth rate can be written as

$$\frac{da}{dN} = C(\Delta K)^m \quad (\text{Eq. 15})$$

with C and m the Paris coefficients, and ΔK the range in stress intensity factor, given by

$$\Delta K = Y \Delta \sigma \sqrt{\pi a} \quad (\text{Eq. 16})$$

where Y is a geometric correction factor and $\Delta\sigma$ is the applied stress range. As initial flaw, we assume that the largest flaw that could have just escaped inspection is present. Typically, this corresponds to a confidence level of 95% and a lower bound population of 90% POD. Like shown on Figure 11, this initial crack is predicted to grow according to (Eq. 15) until it reaches a critical value, corresponding to fatigue failure.

However, if the POS distribution of Figure 10 is superposed onto the graph, it can be seen that the measured value is likely to be an underestimate of the actual flaw size. Hence, the fatigue life predicted by the damage model would not yield a conservative value! When introducing POS data into the calculations, a more accurate lifetime prediction can be made.

5 REFERENCES

- [1] Lewis, E.E., Introduction to Reliability Engineering, 2nd Edition, ISBN 978-0-471-01833-9
- [2] Dover W.D. ;, Brennan F.P., Karé R.F. and Stacey A., Inspection Reliability for Offshore Structures, Proceedings of the 22nd International Conference on Offshore Mechanics and Arctic Engineering, OMEA 2003, Cancun, Mexico, 2003
- [3] Norwegian Ministry of Justice and Police, The Allexander Keilland Accident, Report of the Public Commission, ISBN B000ED27N, 1981
- [4] Clarke M., A Review of the Early Days of Diver Inspection and how Technology has Matured to Greet the Millennium, Offshore Underwater Inspection Insights, vol. 38(6), pp. 395-398, 1996
- [5] Raine G.A, The Development and the Role of Non Destructive Testing in the UK Offshore Industry, Offshore Underwater Inspection Insights, vol. 41(12), pp. 772-777 (1999)
- [6] Raine G.A, The Changing Face of Inspection of Oil and Gas Offshore Installations, Offshore Underwater Inspection Insights, vol. 40(6), pp. 429-434 (1998)
- [7] Van den Abeele F. and Goes P., Electromagnetic Non Destructive Testing Techniques for Defect Sizing of Underwater Welds, Proceedings of the COMSOL Users' Conference, Paris, France, 2010
- [8] Declercq N., Van den Abeele F., Degrieck J. and Leroy O., The Schoch Effect to Distinguish Between Different Liquids in Closed Containers, IEEE Transactions on Ultrasonics, Ferroelectrics and Frequency Control, vol. 51(10), pp. 1354-1357, 2004
- [9] Van den Abeele F., Declercq N., Degrieck J. and Leroy O., The Thomson-Haskell Method to Simulate Bounded Beam Interactions on Layered Media, Proceedings of the 3rd International Conference on Advanced Computational Methods in Engineering, Ghent, Belgium, 2005
- [10] Declercq N. Van den Abeele F., Degrieck J. and Leroy O., On the Use of Bounded Beam Effects to Characterize Fluids in Containers, Proceedings of the 18th International Congress on Acoustics, Kyoto, Japan, 2004
- [11] Satyanarayan L., Sridhar C., Krishnamurthy C.V. and Balasubramaniam K., Simulation of Ultrasonic Phased Array Technique for Imaging and Sizing of Defects using Longitudinal Waves, International Journal of Pressure Vessels and Piping, vol. 84, pp. 716-729, 2007
- [12] Satyanarayan L., Bharat Kumaran K., Krishnamurthy C.V. and Balasubramaniam K., Inverse Method for Detection and Sizing of Cracks in Thin Sections using a Hybrid Genetic Algorithm Based Signal Parametrisation, Theoretical and Applied Fracture Mechanics, vol. 49, pp. 185-198, 2008
- [13] Raine G.A., Review of the Development of the Alternating Current Field Measurement Technique for Subsea Inspection, Offshore Underwater Inspection Insights, vol. 44(12), pp. 748-752, 2002
- [14] Raine G.A., ROV Weld Inspection with a Mid Size ROV and ACFM Array, Offshore Underwater Inspection Insights, vol. 39(6), pp. 409-412, 1997
- [15] Knight M. J., Brennan F.P. and Dover W.D., Effect of Residual Stress on ACFM Crack Measurements in Drill Collar Threaded Connections, NDT&E International, vol. 37, pp. 337-343, 2004
- [16] LeTessier R., Coade R.W. and Geneve B., Sizing of Cracks using the Alternating Current Field Measurement Technique, International Journal of Pressure Vessels and Piping, vol. 79, pp. 549-554, 2002
- [17] Raine G.A., Cost Benefit Applications using the Alternating Current Field Measurement Inspection Technique, Offshore Underwater Inspection Insights, vol. 44(1), pp. 25-30, 2002

- [18]Pachman P.F. et al, Metals Handbook, American Society for Metals, 8th Edition vol. 11, pp. 414-426
- [19]Brennan F. and De Leeuw B., The Use of Inspection and Monitoring Reliability Information in Criticality and Defect Assessment of Ship and Offshore Structures, Proceedings of the ASME 27th International Conference on Offshore Mechanics and Arctic Engineering, OMAE2008, Estoril, Portugal, 2008
- [20]Carvalho A.A., Rebello J.M.A., Souza M.P.V., Sagrilo L.V.S. and Soares S.D., Reliability of Non Destructive Test Techniques in the Inspection of Pipelines used in the Oil Industry, International Journal of Pressure Vessels and Piping, vol. 85, pp. 745-751, 2008
- [21]Dover W.D., Dharmavasan S. Topp D.A. and Lugg M.C., Fitness for Purpose using ACFM for Crack Detection and Sizing and FACTS/FADS for Analysis, Marine Structural Inspection, Maintenance and Monitoring Symposium, Society of Naval Architects and Marine Engineers, Virginia, US, 1991
- [22]British Standards Institution, Guide to Methods for Assessing the Acceptability of Flaws in Metallic Structures, BS 7910, 2005
- [23]American Petroleum Institute, Fitness For Service, API 579-1 / ASME FFS-1, Second Edition, 2007